

The yield of air fluorescence induced by electrons

F. Arqueros*, F. Blanco, A. Castellanos, M. Ortiz, J. Rosado

Departamento de Física Atómica, Molecular y Nuclear, Facultad de Ciencias Físicas, Universidad Complutense, E-28040 Madrid, Spain.

Abstract

The fluorescence yield for dry air and pure nitrogen excited by electrons is calculated using a combination of well-established molecular properties and experimental data of the involved cross sections. Particular attention has been paid to the role of secondary electrons from ionization processes. At high pressure and high energy, observed fluorescence turns out to be proportional to the ionization cross section which follows the Born-Bethe law. Predictions on fluorescence yields in a very wide interval of electron energies (eV - GeV) and pressures (1 and 1013 hPa) as expected from laboratory measurements are presented. Experimental results at energies over 1 MeV are in very good agreement with our calculations for pure nitrogen while discrepancies of about 20% are found for dry air, very likely associated to uncertainties in the available data on quenching cross sections. The relationship between fluorescence emission, stopping power and deposited energy is discussed.

Key words: air-fluorescence, fluorescence telescopes, extensive air showers

1 Introduction

The fluorescence radiation from air showers generated by ultra-high energy cosmic rays UHECRs provides a precise determination of the longitudinal profile allowing the reconstruction of the primary properties. This technique [1] was first successfully used by the Fly's Eye experiment [2] and later by HiRes [3]. Fluorescence telescopes are being used by the Pierre Auger Observatory [4] to operate simultaneously with a giant air shower array. The planned Telescope Array project [5] also relies in this technique. On the other hand, the satellite-based experiments EUSO [6] and OWL [7] are being designed for the detection

* Corresponding author. *e-mail-address:* arqueros@gae.ucm.es

of the fluorescence traces of air showers viewing downward from the top of the atmosphere.

The HiRes collaboration has reported measurements of the energy spectrum of UHECRs [8] which are in disagreement with those of the AGASA air shower array [9]. In order to achieve a reliable energy calibration of a fluorescence telescope, accurate values of the air fluorescence yield are required. This need has promoted a number of experiments for the measurement of this parameter in the wavelength interval of interest in this technique, i.e. 300 - 400 nm. As is well known, in this spectral interval, the fluorescence light comes from the First Negative System of N_2^+ ($B^2\Sigma_u^+ \rightarrow X^2\Sigma_g^+$) and the Second Positive System of N_2 ($C^3\Pi_u \rightarrow B^3\Pi_g$) which in the following will be called 1N and 2P systems respectively.

Kakimoto et al. [10] and Nagano et al. [11], [12] have published measurements of the fluorescence yield using electrons from the β decay of a ^{90}Sr radioactive source (average energy of about 0.85 MeV). Experiments at higher energy are performed using linear accelerators [10], [13], [14], [15]. Finally, measurements at low energy are being carried out with home made electron guns [16]. More information on the status of all these experiments can be found in [17]. On the other hand, the effect of uncertainties in the fluorescence yield on the shower reconstruction are being studied [18] [19].

Electrons passing through the atmosphere deposit energy due to inelastic collisions with air molecules. Only a very small fraction of these processes (i.e. excitation of $B^2\Sigma_u^+$ state of N_2^+ and $C^3\Pi_u$ of N_2) gives rise to the production of fluorescence light in our spectral range. However it is commonly assumed that the fluorescence intensity is proportional to deposited energy. This assumption has not yet been established neither theoretically nor experimentally, at least in a large energy range.

In this paper, the air fluorescence yield is calculated using well known theoretical properties and experimental data on the various cross sections involved in the fluorescence emission. Particular attention has been paid to the role of low energy secondary electrons ejected in molecular ionizations. As a result of our analysis recipes are given which allows the calculation of the absolute value of the total fluorescence yield (pressure and temperature dependent) as a function of electron energy in a wide interval ranging from the threshold to the Gev region. Comparison with available experimental data will be shown.

2 Theoretical considerations

In this section well-established properties on the molecular excitation (by electron collision) and de-excitation are reminded, in particular, the relationship of the fluorescence yield with the excitation cross section and the transition probabilities (radiative and collisional). The contribution of secondary electrons to the fluorescence emission is evaluated. The relationship between deposited energy and fluorescence yield is discussed. All these properties will allow us to make theoretical predictions on the energy dependence of the fluorescence yield.

2.1 Fluorescence yield and optical cross section

Upon passage of an energetic electron through a molecular gas, the *fluorescence yield* for a band $\varepsilon_{vv'}$ is defined as the number of fluorescence photons emitted in the molecular transition $v - v'$ per incident electron and unit path length, where v and v' represent the vibrational quantum numbers of the upper and lower electronic states of the transition respectively. At very low pressures and ignoring secondary processes, $\varepsilon_{vv'}$ is given by

$$\varepsilon_{vv'} = N\sigma_v B^{vv'} = N\sigma_{vv'} \quad (1)$$

where N is the number of molecules per unit volume, σ_v is the excitation cross section for the v level, $B^{vv'}$ is the *branching ratio* (i.e. the ratio between the partial $A_r^{vv'}$ and total A_r^v radiative transition probabilities of the upper level)

$$B^{vv'} = \frac{A_r^{vv'}}{\sum A_r^{vv'}} = \frac{A_r^{vv'}}{A_r^v} \quad (2)$$

and $\sigma_{vv'}$ is the so-called *optical cross section*. As is well known [20], the excitation cross sections σ_v are also approximately proportional to the Franck-Condon factors $q_{X \rightarrow v}$, defined as the overlapping integrals between the vibrational wavefunctions of the lower and upper levels of the transition which in this case are the X ground state of N_2 and the v excited state of N_2 or N_2^+ (depending on the band system) respectively.

Therefore

$$\frac{\sigma_{vv'}}{\sigma_{00}} = \frac{q_{X \rightarrow v}}{q_{X \rightarrow 0}} \frac{B^{vv'}}{B^{00}} \quad (3)$$

The above relation allows the calculation of any optical cross section from data on a reference transition (e.g. σ_{00}). In particular, for the nitrogen molecule the parameters $q_{X \rightarrow v}$ and $B^{vv'}$ are available in the literature [21], [22].

2.2 Quenching, temperature dependence and pollutants effect

At high pressure, molecular de-excitation by collision with other molecules of the medium play an important role (collisional quenching). The corresponding transition probability A_c^v is proportional to the collision frequency and thus to the gas pressure P (assuming fixed temperature). Defining P'_v as the pressure for which the probability of collisional quenching equals that of radiative de-excitation $A_c^v(P'_v) = A_r^v$,

$$A_c^v(P) = A_r^v \frac{P}{P'_v} \quad (4)$$

so the fluorescence yield can be expressed in this case by

$$\varepsilon_{vv'}(P) = N\sigma_v \frac{A_r^{vv'}}{A_r^v + A_c^v(P)} = N\sigma_{vv'} \frac{1}{1 + P/P'_v} \quad (5)$$

The characteristic pressure is given by

$$P'_v = \frac{\sqrt{\pi M k T}}{4\sigma_{nn}} \frac{1}{\tau_r} \quad (6)$$

where M is the molecular mass, k is the Boltzmann's constant, T is the gas temperature and σ_{nn} is the cross section for collisional de-excitation.

Collisional quenching enlarges the total transition probability $A^v = A_r^v + A_c^v$ and therefore the lifetime of the population of excited molecules $\tau^v = 1/A^v$ is shortened as compared with the radiative one $\tau_r^v = 1/A_r^v$ as

$$\frac{1}{\tau^v} = \frac{1}{\tau_r^v} + \frac{1}{\tau_c^v} \quad (7)$$

with $\tau_c^v = 1/A_c^v$. Therefore lifetime depends on pressure as

$$\frac{1}{\tau^v(P)} = \frac{1}{\tau_r^v} \left(1 + \frac{P}{P'_v} \right) \quad (8)$$

Both τ_r^v and P'_v can be measured in a plot of reciprocal lifetime versus pressure (Stern-Volmer plot). This is a very well established technique in use since

many years ago for the experimental determination of radiative lifetimes and quenching cross sections.

For gas mixtures like air, the above formulation is valid taking into account that in equation (1) and (5) N is the density of fluorescence emitters (e.g. nitrogen molecules in air) and the quenching of excited molecules is due to collisions with the various components. Neglecting other components apart from nitrogen and oxygen the P'_v parameter for air is written as

$$P'_v = \frac{\sqrt{\pi M_n kT}}{4\tau_r} \left\{ f_n \sigma_{nn} + f_o \sigma_{no} \sqrt{\frac{M_n + M_o}{2M_o}} \right\}^{-1} \quad (9)$$

where M_n and M_o are the molecular masses of nitrogen and oxygen respectively, σ_{nn} and σ_{no} are the cross sections for collisional quenching of the excited nitrogen with nitrogen and oxygen molecules respectively and f_n y f_o the mass fraction of nitrogen and oxygen in air.

In some media (e.g. plastic scintillators), excited molecules may decay by other additional processes like intersystem crossing or internal conversion [23] and thus the lifetime is further shortened. However for nitrogen (air) gas such internal processes do not take place and therefore they will be neglected in this analysis.

Equations (5) and (9) give the dependence of fluorescence yield with temperature. Firstly, P'_v shows a \sqrt{T} dependence (i.e. collision frequency). On the other hand, the quenching cross sections σ_{nn} and σ_{no} are expected to depend on the kinetic energy of the colliders and therefore a further contribution to the temperature dependence could be expected. Unfortunately no data on this dependence for air in our temperature range is available in the literature and thus this effect, which is not expected to be relevant, will be neglected in our analysis. In fact measurements from the AIRFLY experiment are consistent with quenching cross sections independent on temperature [14].

As is well known oxygen is responsible for the large quenching of air fluorescence as compared with the smaller auto-quenching of pure nitrogen ($\sigma_{no} \gg \sigma_{nn}$). Contribution of other air components (e.g. water vapor) or pollutants can be easily evaluated with equations (5) and the appropriate extension of (9) as far as the corresponding quenching cross sections are available. In this paper quenching by other air components will not be studied.

2.3 Contribution of secondary excitations

Apart from direct excitation by electron collision, the upper level can be populated by de-excitation of higher energy electronic states. This cascading effect contributes to the fluorescence yield enlarging the apparent optical cross sections, so experiments devoted to determine excitation cross sections need to make the appropriate corrections to the measured apparent values. While for our problem, this apparent cross section is the parameter of interest, no significant cascade effects have been reported and so this will be neglected in this analysis.

Pure vibrational transitions (i.e. inside a given electronic state) induced by collisions with other molecules of the medium can redistribute somewhat the population of the upper levels. Very scarce data on this process are available in the literature. However the effect on the total fluorescence yield $\sum_{vv'} \varepsilon_{vv'}$ (i.e. the total number of photons emitted per electron end meter) is expected to be negligible with a possible small effect on the spectrum of the fluorescence radiation. This effect will not be taken into account in our analysis.

A very important secondary contribution will be that from low energy electrons ejected in ionizations. These excite molecular nitrogen increasing the observed fluorescence [24]. As aforementioned, for each primary incident electron of kinetic energy E , the number of direct excitation processes to the v level per unit length is $N\sigma_v(E)$. On the other hand, the number of generated secondary electrons per unit length is $N\sigma_{ion}(E)$ where $\sigma_{ion}(E)$ is the ionization cross section. For our calculations we will use the so-called gross ionization cross section which also includes processes in which more than one electron is generated in a primary interaction (even though contribution from those processes is small). If we name $\alpha_v(E, P)$ the fraction of these secondary electrons that excite the upper v level ($\alpha_{vv'} = \alpha_v B^{vv'}$ the fraction that excites $v - v'$ band emission), then an effective optical cross section $\sigma_{vv'}^{eff}$ can be defined as

$$\sigma_{vv'}^{eff} = \sigma_{vv'}(E) + \alpha_{vv'}(E, P)\sigma_{ion}(E) \quad (10)$$

and the total fluorescence yield given by equation (5) becomes

$$\varepsilon_{vv'}(P) = N \frac{1}{1 + P/P_v'} \sigma_{vv'}^{eff} \quad (11)$$

The effect of these secondary electrons results the dominant mechanism for the production of 2P fluorescence at high pressure [24]. In addition, as will be shown in sub-section 3.1, a non-negligible contribution of the 1N fluorescence is due to these secondary electrons.

The $\alpha_{vv'}$ parameter can be calculated by means of a Monte Carlo simulation. For this work the simple algorithm described in [24] has been used with a somewhat improved treatment of the electrons escaping the interaction region. The resulting small dependence of $\alpha_{vv'}$ on primary electron energy, pressure and characteristic size of interaction region R , can be approximated (for 1hPas and higher pressures) by

$$\alpha_{vv'}(E, P) = \min\{s_0 \ln \frac{P \times R}{s_1}, e_0 \ln \frac{E}{e_1}\} \quad (12)$$

The value of the s_0 , s_1 , e_0 and e_1 parameters depend on the particular case. Results for 0-0 bands of 1N and 2P systems are shown in table 1. A paper describing the details of the abovementioned improvements for this model is in preparation [25].

Since $\alpha_{vv'}$ is proportional to the corresponding optical cross section, expression (3) leads to

$$\frac{\alpha_{vv'}}{\alpha_{00}} = \frac{q_{X \rightarrow v}}{q_{X \rightarrow 0}} \frac{B^{vv'}}{B^{00}} \quad (13)$$

which allows the calculation of the various $\alpha_{vv'}(E, P)$ parameters from α_{00} .

	s_0	s_1 (hPa \times cm)	e_0	e_1 (eV)
1N (0-0)	$8.67 \cdot 10^{-3}$	$1.92 \cdot 10^{-2}$	$1.37 \cdot 10^{-2}$	73.7
2P (0-0)	$2.00 \cdot 10^{-3}$	$1.36 \cdot 10^{-5}$	$3.22 \cdot 10^{-3}$	0.942

Table 1.- *Values of the parameters in equation (12) for the most prominent bands of the 1N and 2P molecular systems.*

Note that experiments determining quenching cross sections from the pressure dependence of fluorescence intensity may overestimate the P' values if they ignore the effect of secondary electrons by using equation (5) instead of the (11) right one. As mentioned above the P' parameter can be also measured in a plot of reciprocal lifetime versus pressure. This is a safe technique not affected by secondary electrons.

2.4 Stopping cross section and deposited energy

The stopping power for electrons S , i.e. the energy loss per unit length of traversed matter due to both excitation and ionization processes, can be ac-

curately determined for energies above 1 keV by the well known Bethe-Bloch formula [26]. At lower energy, experimental results are available down to 25 eV [27]. On the other hand, in general, S can be expressed [20] as

$$S = \frac{dw}{dx} = N \sum E_n \sigma_n \quad (14)$$

where the summation includes the energy E_n and cross section σ_n for all kinematically accessible excited states n (ionization processes contributing there with a large family of continuum states). The cross section σ_n depends on the electron incident energy, and can be determined in electron scattering experiments [28]. A *stopping cross section* $\sigma_{st}(E)$, proportional to S , can be easily defined [20] by rewriting (14) as

$$S = \frac{dw}{dx} = NR_y \sum (E_n/R_y) \sigma_n = NR_y \sigma_{st} \quad (15)$$

where R_y is the Rydberg constant (13.606 eV). This $\sigma_{st}(E)$ cross section, proportional to the stopping power, will be useful for comparison purposes in the present analysis.

The *fluorescence efficiency* $\Phi_{vv'}$ is defined as the fraction of deposited energy which is emitted as photons of the $v - v'$ band. Slow electrons deposit all the energy locally and thus the Bethe-Bloch formula gives the dependence of deposited energy on E . Therefore for low energy electrons

$$\Phi_{vv'}(P) = \frac{E_{vv'} \varepsilon_{vv'}}{dw/dx} = \frac{E_{vv'} \sigma_{vv'}}{R_y \sigma_{st}} \frac{1}{1 + P/P'_v} \quad (16)$$

Note that the interpretation of the fluorescence efficiency given by some authors [1], [11] is different from that of equation (16). These authors assume that all the electron energy loss is employed in the excitation of the molecules to one single upper level, a fraction is supposed to be emitted as fluorescence radiation and the remaining energy is lost by internal quenching. Such a model which is valid in some media (e.g. plastic scintillators) [23] is not applicable in our case. In fact, only a small fraction of the lost energy is used in the excitation of the level v of interest while the remaining energy gives rise to other direct excitations, not internal processes.

At high energy the stopping power also accounts for the production of high energy secondary electrons which do not deposit their energy locally (large range and bremsstrahlung emission). Unless the interaction region (e.g. gas cell in a lab experiment) is very large, a non-negligible fraction of the energy transferred to the medium by the primary electron is not deposited inside the

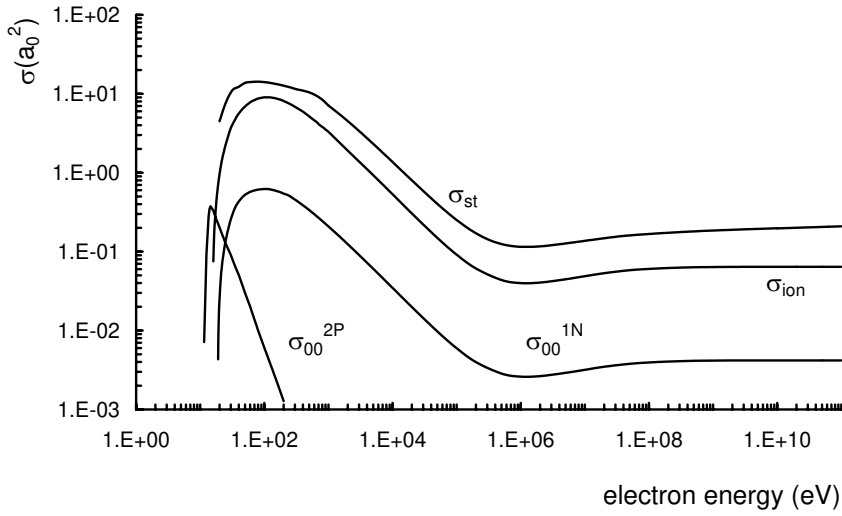


Fig. 1. Cross sections (atomic units) involved in the emission of fluorescence as a function of energy for air at atmospheric pressure. The optical cross section σ_{00}^{1N} for the 1N system has been obtained from experimental data at low energy assuming a Born-Bethe behavior at high energy and including the density correction (see 3.1). The ionization cross section σ_{ion} has been taken from [48]. Experimental results have been used for the 2P optical cross section σ_{00}^{2P} (see 3.2). The σ_{st} cross section (proportional to the electron stopping power) has been obtained from [26] and [27] for energies above and below 1 keV respectively.

volume and consequently a non-negligible fraction of the fluorescence radiation is not emitted in the interaction region.

According to equation (11), several terms contribute to the total fluorescence yield. At low energy and low pressure the main contribution is direct excitation. In principle the energy dependence of σ_{st} and $\sigma_{vv'}$ are not expected to be the same since σ_v excitation cross section only accounts for one of the many inelastic processes involved in the energy loss. On the other hand, even if σ_n followed the same behavior for all processes (including those leading to the generation of fluorescence light) $\varepsilon_{vv'}$ is not expected to be proportional to σ_{st} because of the different weighting values of E_n in equation (15) depending on each particular process. In figure 1 the cross sections involved in fluorescence emission and energy deposition are shown as a function of energy for comparison. For instance, the different behavior of σ_{st} and 2P optical cross section is evident.

As shown in detail later, at high energy and high pressure the fluorescence yield is approximately proportional to the ionization cross section which follows the Born-Bethe relativistic law [20]. The Born-Bethe law for the electron-molecule

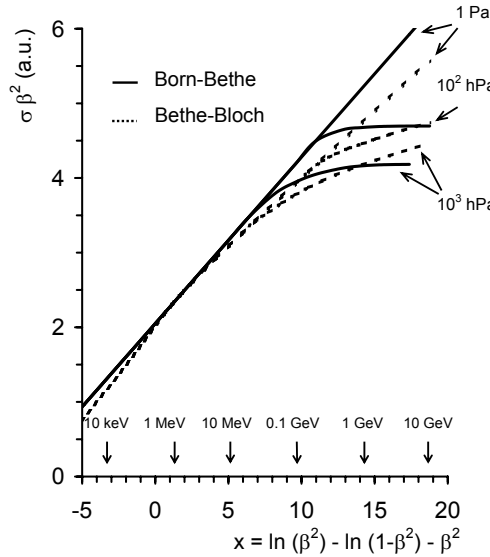


Fig. 2. Comparison on a Fano plot of the stopping cross section (Bethe-Bloch) and the ionization cross section (Born-Bethe) for air at 1Pa, 100 hPa and atmospheric pressure. Cross sections (in arbitrary units) have been normalized in order to get a common value at 1 MeV for all cases. Pure Born-Bethe function (e.g. ionization cross section at 1Pa) is linear while the Bethe-Bloch stopping cross section clearly deviates from linearity. Density effect tends to saturate both functions at high energy although the effect is more pronounced for the ionization cross section.

collision can be expressed as

$$\sigma = \frac{A}{\beta^2} \{ \ln C \beta^2 - \ln(1 - \beta^2) - \beta^2 \} \quad (17)$$

where β is the relativistic speed and, A and C are constants. At very high energies, a density correction has to be applied to take into account the polarization of the molecules along the electron path [29], [30], [31]. For that purpose, we have included the density correction in the transversal contribution of the Born-Bethe expression [20], in the form proposed by [29]. The resulting expression turns out to be

$$\sigma = \frac{A}{\beta^2} \{ \ln C \beta^2 - \ln(1 - \beta^2) - \beta^2 - \delta_F \} \quad (18)$$

where δ_F is the usual density correction parameter included in the Bethe-Bloch formula for the stopping power [32]. Because of this density correction, the ionization cross section of the nitrogen molecule at high energy depends on pressure.

For any pure Born-Bethe cross section (17), $\sigma\beta^2$ versus $x = \ln(\beta^2) - \ln(1 - \beta^2) - \beta^2$ is a straight line (the so-called Fano plot). In figure 2 the ionization cross section has been represented on a Fano plot for several pressures together with the corresponding stopping cross section (Bethe-Bloch formula) [33]. As expected, at very low pressure, σ_{ion} follows a linear behavior while σ_{st} clearly deviates from linearity. At high pressure and very high energy both functions flattens as expected from the density effect but following a slightly different behavior.

At low energy σ_{st} is not proportional to σ_{ion} and therefore we can conclude that fluorescence yield is not expected to be exactly proportional to deposited energy since most of the fluorescence radiation is generated by low energy electrons (either primaries or secondaries) for which fluorescence emission and stopping power follow different energy behavior.

3 The fluorescence yield in pure nitrogen and dry air

In this section experimental data on the excitation/de-excitation of the upper levels of the 1N and 2P systems of nitrogen will be analyzed. This information will allow us the evaluation of the fluorescence yield.

3.1 The First Negative system

The 1N system of N_2^+ has been studied by many authors. In particular many measurements of the optical cross section σ_{00} corresponding to the strongest band at 391.2 nm are available in the literature. At very low energies, absolute measurements have been reported by Borst and Zipf [34] (19 eV $< E <$ 3.0 keV), Stanton and St John [35] (19 eV $< E <$ 400 eV), Aarts et al. [36] (97 eV $< E <$ 6 keV), Srivastava and Mirza [37] (70 eV $< E <$ 4 keV), Holland [38] (90 eV $< E <$ 2 keV), McConkey and Latimer [39] (26 eV $< E <$ 300 eV) and McConkey et al. [40] (18 eV $< E <$ 2 keV). In figure 3 a significant set of the above measurements have been represented on a Fano plot. Also, relative measurements published in [41], normalized to an average value of the above authors in the overlapping region, have been included.

At higher energies some measurements are available. Data of O'Neil and Davidson in the range 3 - 60 keV [42] are shown in the figure. Cross sections inferred from previous measurements of these authors with 50 keV electrons at high pressure [43] are significantly smaller and they will not be used in the present analysis. As shown in the figure, the above measurements follow a linear behavior in a Fano plot. Note that the density correction is only rele-

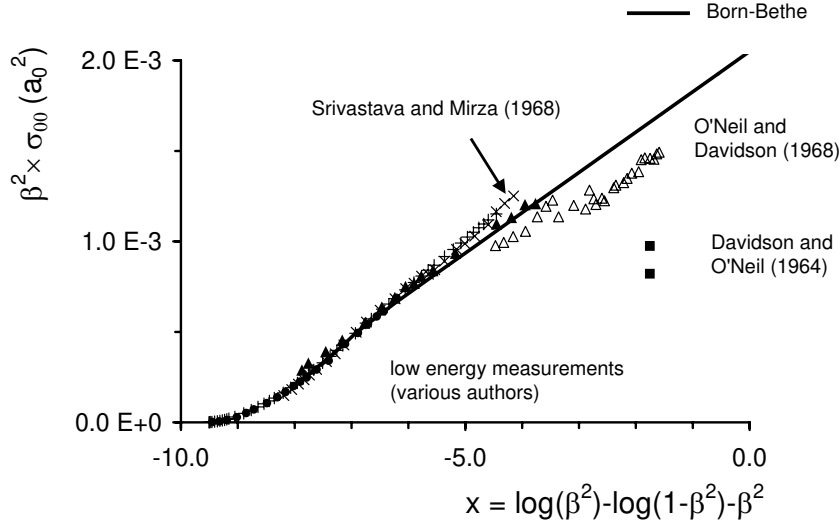


Fig. 3. Fano plot for the optical cross section σ_{00} (in atomic units) of the 1N system. Experimental results (symbols) show a linear behavior at energies over about 150 eV. Discrepancies in the slope are very likely due to calibration factors. An average linear fit (continuous line) has been used in this work for the calculation of the 1N fluorescence yield.

vant at very high energy. The slope of the various data sets, i.e. A parameter in equation (17), have slightly different values while a reasonable agreement in the abscise in the origin is found, i.e. C parameter. This features can be interpreted as discrepancies in the absolute calibration factors of the various experiments, while their results agree in the shape of the $\sigma_{00}(E)$ function.

An average linear fit of the available data to equation (17) is shown in figure 3. The values of the parameters were found to be $A = 2.230 \times 10^{-4} a_0^2$ and $C = 9.826 \times 10^3$. None of these experimental works reports any contribution of cascades to the measured optical cross section. As a further test of the absence of cascades, it has been checked [24] that the measured optical cross sections of this system fulfills equation (3). Therefore the above Born-Bethe function provides us with a reliable value of σ_{00} in the whole energy range (see figure 1). Note that at very high energy the density correction has to be included. Optical cross section for other 1N bands can be easily obtained using relation (3).

While at very low pressures and low energies $\sigma_{vv'}$ values suffice for evaluating fluorescence yields by means of equation (1), at those conditions we are interested here, quenching and secondary-electron contributions have to be considered by means of equation (11). Expression (12) and table 1 show that the α_{00} parameter, accounting for the contribution of secondary electrons of

the most intense band of the 1N system (391.2 nm), ranges from 0 (at low E and/or low $P \times R$ conditions) to 0.12 (at $E = 1\text{Mev}$ and $P \times R = 5 \text{ atm} \times \text{cm}$). In order to appraise the importance of these secondary contributions it must be noted that $\sigma_{00} \simeq 0.075\sigma_{ion}(E)$ for 1N system at large energies (see figure 1). Introduction of that result in equation (11) reveals that secondary/direct contributions are in the $\alpha_{00}/0.075$ ratio and thus, contributions from secondary electrons can be very important at high pressures and high energies.

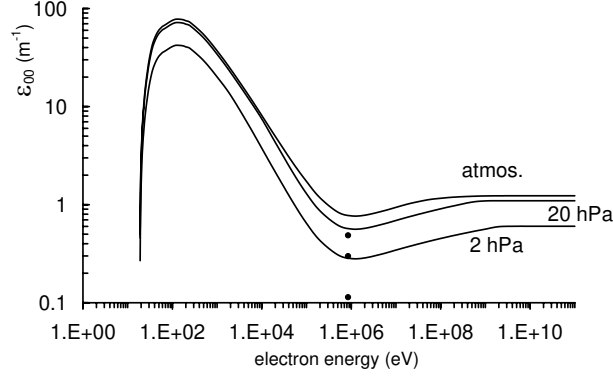


Fig. 4. Fluorescence yield of the most prominent band of the 1N System (391.2 nm) for pure nitrogen at several pressures. Predictions of this work (continuous line) are compared with experimental data of Nagano et al. [12] (●) at the same pressures.

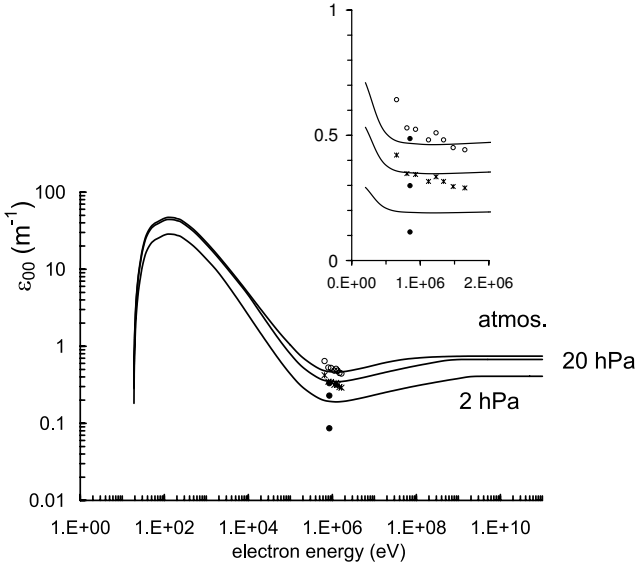


Fig. 5. Same as figure 4 for dry air. In addition, experimental values of Hirs et al. [44] at 20 hPa (x) and atmospheric pressure (○) are shown for comparison (see the inset for a more detailed comparison).

The above results allow the calculation of ε_{00} as a function of electron energy, pressure, temperature and characteristic size of the interaction region in a

given experimental arrangement. As an example figures 4 and 5 show $\varepsilon_{00}(E)$ for pure nitrogen and dry air respectively, in a wide energy range (eVs - GeVs) for several pressures (2, 20 and 1013 hPa) and a temperature of $T = 300$ K. Characteristics pressures of $P'_0 = 1.7$ and 1.3 hPa for pure nitrogen and dry air respectively have been assumed (see sub-section 3.3 for a discussion on available P' values). In these calculations a characteristic size of $R = 2.5$ cm has been assumed, which can be considered as representative for typical lab measurements. The fluorescence yield results of Hirs et al.[44], for dry air, and Nagano et al. [12], for both nitrogen and dry air, are shown in the figures for comparison. Direct measurements of [44] are in agreement with our predictions showing that our correction for secondary electrons accounts for these experimental results. On the contrary, our calculations are in clear disagreement with measurements of [12] for which a two line analysis had to be applied in order to subtract the contribution of other band not separated by the spectroscopy filter. As shown below, the contribution of the 1N system to the total air fluorescence yield (at high pressure) is in the range of 15% and therefore the above discrepancy is not so relevant for the total fluorescence yield.

3.2 The Second Positive system

Fluorescence of the 2P system in both pure nitrogen and air has been extensively studied by many authors. Experiments aiming at measuring the electron excitation cross section of the upper level $C^3\Pi_u$ carried out on pure nitrogen at low electron energy ($E < 1$ keV) and low pressure (a few mTorr or lower) show a fast E^{-2} dependence of the fluorescence light [45], [46], [47] much faster than that of the 1N system. This result is expected, taking into account the optically-forbidden nature of the 2P transition. In figure 1 the optical cross section for the 0 – 0 band of the 2P system from the abovementioned measurements is shown.

Since at 1 keV energies, 2P fluorescence observed at low pressure is much weaker than that of the 1N system, a naive extrapolation would predict that the 2P fluorescence should be completely negligible compared to 1N one at 30 keV energies and above. On the contrary experiments [10], [11], [12], [43] carried out at high energies (up to 1 GeV) on air at high pressure (ranging from a few hPa up to 1 atm) shows that the 2P fluorescence even dominates over the 1N system. This feature can be explained taking into account the effect of the secondary electrons ejected in ionization processes [24]. The contribution of these secondary electrons have been evaluated from a MC calculation as explained above and the values of the corresponding parameters of expression (12) for the most intense band of this system (337.0 nm) are shown in table 1.

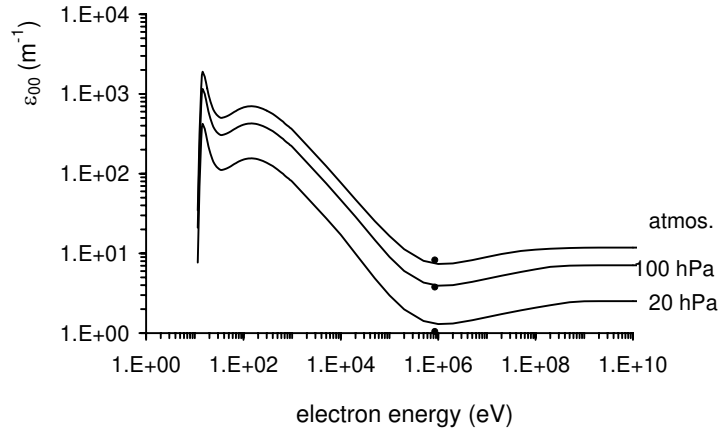


Fig. 6. *Fluorescence yield of the most prominent band of the 2P System (337.0 nm) for pure nitrogen at several pressures. Predictions of this work (continuous line) are compared with experimental data of Nagano et al. [12].*

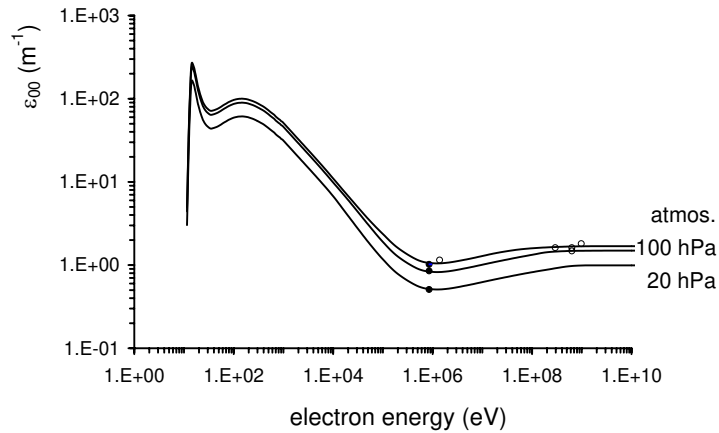


Fig. 7. *Same as figure 6 for dry air. In addition experimental results of Ueno [13] at atmospheric pressure (o) are shown.*

Characteristic pressures of $P'_0 = 77$ and 13.1 hPa for pure nitrogen and dry air respectively have been assumed (see below for a discussion on available P'_v values). Figures 6 and 7 show the predicted fluorescence yield for the 0-0 band of the 2P system as a function of electron energy from threshold (eVs) up to the GeV region at several pressures in pure nitrogen and dry air respectively. An interaction region of 2.5 cm radius has also been assumed for this calculation. Experimental data for the 337.0 nm band at 0.85 MeV [12], 1 MeV and near 1 GeV [13] are shown for comparison.

3.3 Total fluorescence yield

The total fluorescence yield, i.e. the sum of the contributions from all the molecular bands of both systems 1N and 2P,

$$\varepsilon = \sum_{vv'} \varepsilon_{vv'}^{1N} + \sum_{vv'} \varepsilon_{vv'}^{2P} \quad (19)$$

can be easily calculated from (11) provided that the involved molecular parameters are available for all transitions. Taking into account (3) and (13) the contribution of each band system to the total fluorescence yield can be expressed as a function of a reference transition (e.g. 0-0) as

$$\varepsilon^{system} = N \frac{\sigma_{00}^{eff}(E, P)}{q_{X \rightarrow 0} B^{00}} \sum_{vv'} q_{X \rightarrow v} B^{vv'} \frac{P'_v}{P + P'_v} = N \frac{\sigma_{00}^{eff}(E, P)}{q_{X \rightarrow 0} B^{00}} \sum_v q_{X \rightarrow v} \frac{P'_v}{P + P'_v} \quad (20)$$

where (2) has been used. All the parameters depend on the system, 1N or 2P. The terms inside the v-v' sum represent the relative intensities of the bands for the corresponding system and at high pressures ($P \gg P'_v$) they can be approximated by

$$\varepsilon_{vv'} \sim q_{X \rightarrow v} B^{vv'} P'_v \quad (21)$$

In general, equation (21) is able to predict experimental results on relative intensities although a detailed comparison is beyond the scope of this paper.

v / v'	0	1	2	3	5	5	$q_{X \rightarrow v}$	P_{nitr}^v (hPa)	$P_{air}^{v'}$ (hPa)
0	391.2	427.5	470.6	522.5	586.1	665.9			
	0.627	0.204	0.043	0.007	0.001	0.000	0.883	1.7	1.3
1	358.0	388.2	423.4	464.9	514.6	575.0			
	0.041	0.029	0.030	0.011	0.003	0.001	0.114	—	—
2	330.5	356.1	385.5	419.7	459.7	570.4			
	0.000	0.001	0.000	0.000	0.000	0.000	0.002	—	—

Table 2.- Molecular parameters for the 1 N system. Each box of the vv' table shows the wavelength (nm) of the v-v' transition (upper number) and the product $B^{vv'} \cdot q_{X \rightarrow v}$ (lower number). The horizontal sum of these products is equal to the $q_{X \rightarrow v}$ Franck-Condon factor for the molecular excitation. Last two rows show the values of the characteristic pressures for the quenching of the upper v level in pure nitrogen and air (see text for more details).

v / v'	0	1	2	3	4	5	6	7	8	$q_{X \rightarrow v}$	$P_{nitrogen}'$ (hPa)	P_{air}' (hPa)
0	337.0	357.6	380.4	405.8	434.3	466.5	503.2	545.2	593.8	0.545	77	13.1
	0.265	0.175	0.072	0.022	0.006	0.001	0.000	0.000	0.000			
1	315.8	333.8	353.6	375.4	399.7	426.8	457.3	491.7	530.9	0.308	36	11.2
	0.138	0.007	0.064	0.057	0.028	0.010	0.003	0.001	0.000			
2	297.6	313.5	330.9	349.9	370.9	394.2	420.0	448.9	481.3	0.106	23	9.1
	0.016	0.041	0.003	0.007	0.016	0.013	0.006	0.002	0.001			
3	281.8	296.2	311.5	328.4	346.8	367.1	389.4	414.0	441.5	0.030	22	7.9
	0.001	0.009	0.007	0.003	0.000	0.003	0.004	0.002	0.001			
4	268.4	281.2	295.2	310.2	326.6	344.5	364.1	385.6	409.3	0.008	21	6.7
	0.000	0.000	0.003	0.001	0.001	0.000	0.000	0.001	0.001			

Table 3.- Same as table 2 for the 2P system.

Values for the involved parameters are shown in tables 2 and 3 for 1N and 2P systems respectively. Accurate Franck-Condon factors $q_{X \rightarrow v}$ and branching ratios $B^{vv'}$ have been taken from [21]. In regard with the characteristic pressures P'_v , many measurements are available in the literature.

For the 1N system [1], [12] and [49] provide experimental results for the $v=0$ level for both pure nitrogen and dry air. A reasonable agreement between [1] and [49] is found and an average value of both results, shown in table 2, has been used in our calculations. Since no results for $v > 0$ seems to be available, the same P'_0 value has been used for all v levels. The bands of this system are strongly attenuated by quenching and therefore their contribution at high pressure is very small, consequently, even a severe error in P'_v ($v > 0$) would not have a significant effect on the calculated total fluorescence yield.

On the other hand, quenching of the 2P system by nitrogen (auto-quenching) has been extensively studied by many authors [1], [12], [49], [52], [53], [54], [55], [56], [57], [58], [59], [60], [61], [62], [63]. Unfortunately large discrepancies between the various measurements are found. Averaged values from [58], [59] and [60], in good agreement with a significant fraction of previous measurements, have been used in this work (see table 3).

The total fluorescence yield for the bands contributing to the usual experimental spectroscopic interval (300 - 406 nm) has been evaluated as a function of electron energy and pressure. Note that expression (20) had to be corrected to account for the missed transitions (those outside the above wavelength limits). A plot of $\varepsilon(E)$ for pure nitrogen in the interval ranging from threshold to the GeV region at several pressures ranging from 1 hPa to atmospheric pressure is shown in figure 8. Several interesting features of $\varepsilon(E, P)$ can be observed in this figure. At high pressure, expression (20) becomes

$$\varepsilon^{system} = \frac{1}{kT} \frac{\sigma_{00}^{eff}(E, P)}{q_{X \rightarrow 0} B^{00}} \sum_v q_{X \rightarrow v} P'_v \quad (22)$$

showing that for $P \gg P'_v$ the fluorescence yield is basically independent on pressure. The only remaining dependence is the small one from the α parameter and (even smaller) that from the density correction of σ_{ion} at high energy. That is, the increase of fluorescence with pressure is nearly canceled out by the corresponding increased quenching. Note that the higher is P'_v , the weaker is the pressure dependence of fluorescence yield.

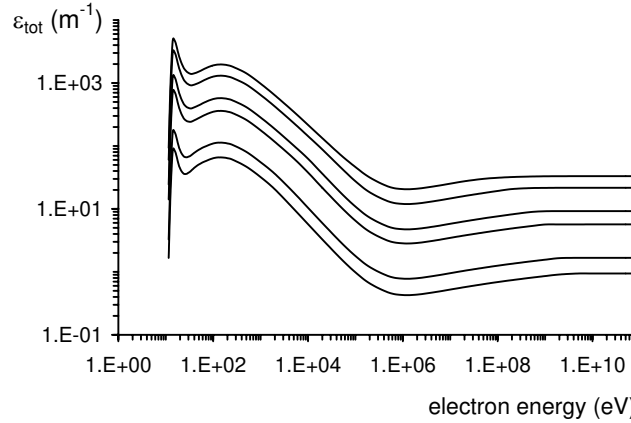


Fig. 8. Total fluorescence yield (300 - 406 nm) versus energy for pure nitrogen at pressures (bottom - up) 1, 2, 10, 20, 100 and 1013 hPa for a characteristic size of the interaction region of $R = 2.5$ cm.

The σ_{00}^{eff} parameter can be easily evaluated. For energies about 100 eV and over, the optical cross sections of the 1N system are proportional to the total ionization cross section, $\sigma_{00}^{1N}(E) = \chi_{00}\sigma_{ion}(E)$ and therefore

$$\sigma_{00}^{1N,eff}(E, P) = (\chi_{00} + \alpha_{00}^{1N})\sigma_{ion} \quad (23)$$

In regard with the 2P system the contribution of direct excitation at high energy and high pressure ($E \gtrsim 10^3$ eV and $P \times R \gtrsim 3$ hPa \times cm) is negligible because under these conditions $\sigma_{vv'} \ll \alpha_{vv'}\sigma_{ion}$ and thus

$$\sigma_{00}^{2P,eff}(E, P) \approx \alpha_{00}^{2P}\sigma_{ion} \quad (24)$$

The $\alpha(E, P)$ parameter reaches saturation (i.e. it becomes independent of E for increasing energies) at an energy which grows with pressure (12). The data in table 1 shows that this saturation energy results of about 10^4 eV (10^5 eV) for the 2P (1N) system at atmospheric pressure. As a consequence for higher energies $\varepsilon(E)$ is proportional to $\sigma_{ion}(E)$.

The results of our calculations have been compared with available experimental data. Figure 9 shows the total fluorescence yield (300 - 406 nm) at high energy and atmospheric pressure for pure nitrogen together with the absolute

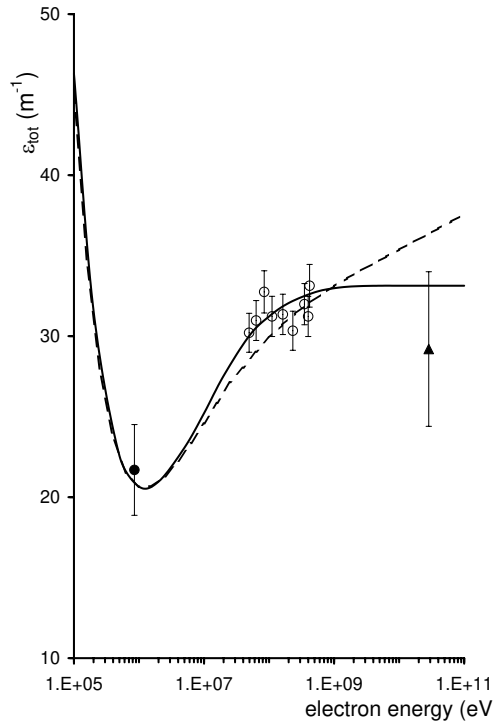


Fig. 9. Total fluorescence yield (300 - 406 nm) at high energy for pure nitrogen. Predictions of this work (continuous line) are compared with absolute measurements of Nagano et al. [12] (\bullet) and the FLASH collaboration [15] (\blacktriangle). Relative measurements of AIRFLY (\circ) normalized to our predictions at 10^8 eV are also shown. Dashed line represents the Bethe-Bloch function normalized at 1 MeV.

measurements of Nagano et al. [12] at 0.850 MeV and those of the FLASH collaboration [15] at 28.5 GeV. In addition, relative measurements of AIRFLY [14] in the interval 50 - 500 MeV have been represented. As shown in the figure, experimental data for pure nitrogen are in good agreement (within the experimental errors) with our predictions.

Unfortunately, quenching measurements in air for the 2P system are scarce, showing also large discrepancies. Bunner [1] gives P'_v values of 20 and 8.7 hPa for $v = 0$ and 1 respectively. Nagano et al [12] measure P' values from the fitting of experimental $\varepsilon(P)$ results. Average values of about 18, 25 and 8 hPa are found for $v = 0$, 1 and 2 respectively. As already mentioned these P'_v values could be overestimated by the contribution of secondary electrons. Finally, Pancheshnyi et al. [59] have published measurements of the Nitrogen 2P quenching by O₂ molecules in good agreement with the results of [63] and [54]. These measurements give the air P'_v values shown in table 3 which have been used in our calculations.

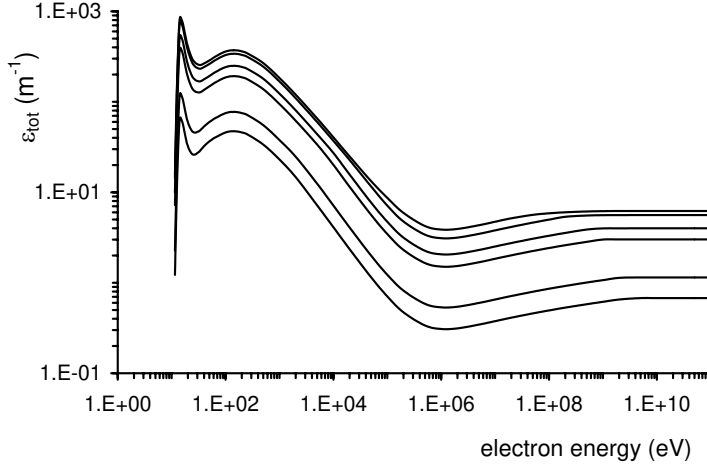


Fig. 10. Total fluorescence yield (300 - 406 nm) for dry air against electron energy at pressures (bottom-up) 1, 2, 10, 20, 100, 1013 hPa for a characteristic size of the interaction region of $R = 2.5$ cm.

Figure 10 shows plots of $\varepsilon(E)$ for dry air in a wide energy interval for several pressures ranging from 1 hPa to atmospheric pressure. In figure 11 these results are compared with available measurements at high energy. Our calculations are in good agreement with that of Nagano et al. [12] at 0.850 MeV but they predict a fluorescence yield about 20% larger than the measurements of Kakimoto et al. [10] (at several energies in the range 1 MeV - 1GeV) and those of the FLASH collaboration [15] at 28.5 GeV.

The calculations presented in this work relies in several molecular parameters and in a model for evaluating the contribution of secondary electrons. Branching ratios, Franck-Condon factors and the validity of the Franck-Condon principle are reliable and thus their contribution to the uncertainty in ε is expected to be very small. On the other hand, at high pressure, fluorescence yields are proportional to P'_v values for which large discrepancies are found in the available measurements. The uncertainty in these parameters are very likely one of the main error sources in our calculations. On the other hand, our model [24], [25] uses several molecular parameters which can also contribute to a systematic error in the evaluation of the fluorescence light from secondary electrons, in particular, the absolute value of the total excitation cross section of N_2 . This uncertainty leads to a possible (small) constant factor error. On the contrary, the geometry of the interaction volume (different for the various experiments) should not contribute significantly to our errors since $\alpha_{vv'}$ grows very slowly with R ($\approx \ln R$). In regard with the energy dependence, our calculations rely in the validity of the well established Born-Bethe approximation at high energy.

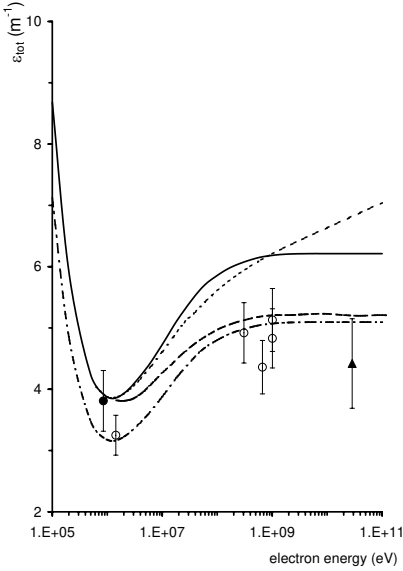


Fig. 11. Total fluorescence yield (300 - 406 nm) at high energy for dry air. Continuous line represents the prediction of this work using the parameters of tables 2 and 3. The comparison with experimental results of Nagano et al. [12] (●), Kakimoto et al. [10] (○) and the FLASH collaboration [15] (▲) suggests that P'_v values could be overestimated (see text for more details). Results of this work reduced by 18% (dash-dotted line) are in good agreement with all measurements. Dotted line represents the stopping power and the dashed line is the deposited energy from [15] both normalized to ε at 1 MeV.

In summary, at high pressure the predictions of this work could be affected by a small error (constant factor) mainly due to the uncertainty in the quenching efficiency. In figure 11 our fluorescence yield reduced by a constant factor of 18% has been plotted showing a reasonable agreement with all experimental results. Note that the ratio of fluorescence yields $\varepsilon^{air}/\varepsilon^{nitrogen}$ in experiments measuring both gases (air and nitrogen) at high pressure are expected to be equal to the ratio $P'_{air}/P'_{nitrogen}$ since experimental errors (calibrations, geometrical factors, etc.) are the same for both gases. Our predictions for nitrogen agree with the absolute measurements of [12] and [15] while a fluorescence efficiency about 20% larger than [10] and [15] is predicted for air. This lead us to suspect that the ratio $P'_{air}/P'_{nitrogen}$ assumed in our calculations has been overestimated by about a 20%.

In figures 9 and 11 a plot of the stopping power law for electrons (Bethe-Bloch) has been represented showing a noticeable deviation with respect to $\varepsilon(E)$ as predicted, since at large E values a significant fraction of the electron energy loss is not deposited inside the fluorescence cell. At low energy the fluorescence yield also deviates from the stopping cross section as shown in figure 12. As already mentioned most of the fluorescence light is generated

by low energy secondary electrons for which deposited energy is proportional to the stopping cross section. Since at low E , ε/σ_{st} is energy dependent, the ε to deposited energy ratio is expected to depend on E at high energy also. In figure 11 the deposited energy versus E reported by [15] for the FLASH experiment has been also represented (normalized to our fluorescence yield at 1 MeV). Our calculations predict that at large energies a growing fraction of deposited energy is converted in fluorescence radiation. According to this figure, the ratio ε to deposited energy grows about 19% in the interval 1 MeV - 1 GeV.

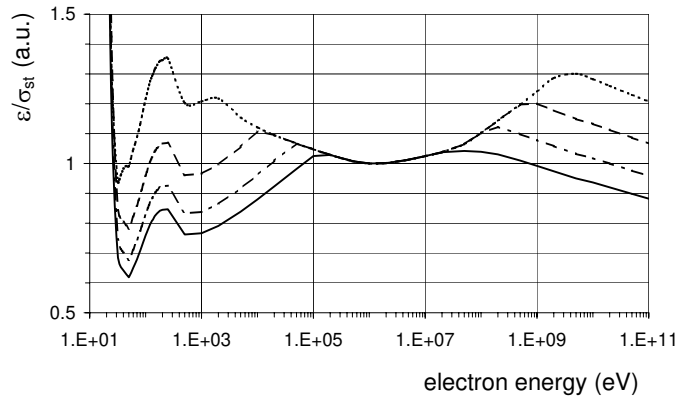


Fig. 12. Ratio of fluorescence yield over stopping cross section (Bethe-Bloch) for air (arbitrary units) at 1 hPa (dotted), 20 hPa (dashed), 200 hPa (dot-dashed) and 1013 hPa (continuous). The ratio has been normalized to 1 at 1MeV.

4 Conclusions

Theoretical predictions on the fluorescence generation of nitrogen molecules excited by electrons have been presented. A general procedure for the calculation of fluorescence yields is shown which can be applied in a very wide energy interval ranging from threshold up to the GeV region and for any environmental condition (pressure, temperature, contaminants, etc.) as far as the involved molecular parameters are available. As an example, plots of fluorescence yields (as expected from typical laboratory experiments) versus energy in a wide pressure range are shown.

The contribution of direct excitation of 1N system is calculated using low energy measurements of the optical cross section with extrapolation to high energies as given by the Born-Bethe law. Direct excitation of 2P system is negligible. Particular attention has been paid to the the contribution of secondary electrons ejected in ionization processes. A simple model is used to

evaluate the fluorescence from secondary electrons which turns out to be non-negligible for the excitation of the 1N system and dominant for the generation of the 2P fluorescence. At high energy and high pressure fluorescence yield results proportional to the total ionization cross section which also follows a Born-Bethe energy law. Quenching of fluorescence by N_2 and O_2 molecules is taken into account using available data in the literature. At high pressure, fluorescence yield is proportional to the P'_v parameters. Unfortunately values of these parameters reported in the literature show large disagreements.

Comparison of our predictions with available measurements at high energy ($E > 1\text{MeV}$) and high pressure shows very good agreement for pure nitrogen while some discrepancies of about 20% are found for dry air. These discrepancies are very likely due to uncertainties in the quenching cross sections.

The relationship between fluorescence yield, stopping power and energy deposited by the electrons in the medium has been discussed. In a typical laboratory experiment, at very high energy, many secondary electrons reach the wall of the cell before emitting all the fluorescence light and therefore stopping power grows with energy faster than fluorescence yield. On the other hand, most of the fluorescence light is generated by low energy secondary electrons for which the optical cross section is not proportional to the stopping power and therefore, in principle, proportionality between fluorescence yield and deposited energy is not assured. A comparison of our fluorescence yield results with deposited energy in the FLASH experiment shows a deviation from proportionality of about 20% in the interval 1 MeV - 10 GeV.

More details on the model used in this work for the evaluation of the fluorescence contribution of secondary electrons will be published soon. On the other hand a detailed study on the relationship between deposited energy and fluorescence yield following our model is underway.

Acknowledgments

This work has been supported by the Spanish Ministry of Science and Education MEC (ref.: FPA03-08733-C02-01). A.Castellanos acknowledges an undergraduate grant from the program “Becas Colaboración” of MEC

References

- [1] A.N. Bunner, Ph.D. thesis, Cornell University, 1967.
- [2] R.M. Baltrusaitis et al., Nucl. Instrum. Meth. Phys. Res. A 240 (1985) 410.
- [3] T. Abu-Zayyad et al., Nucl. Instrum. Meth. Phys. Res. A 450 (2000) 253 - 269.
- [4] J. Abraham et al. (Pierre Auger Collaboration), Nucl. Instrum. Meth. Phys. Res. A 523 (2004) 5095; J. A. Bellido et al., 29th Int. Cosmic Ray Conf. (Pune) 7 (2005) 13.
- [5] M. Fukushima, Prog. Theor. Phys. Suppl. 151 (2003) 206
- [6] O. Catalano et al., Nuovo Cim. Soc. Ital. Fis., 24C (2001) 445.
- [7] F.W. Stecker et al., Nucl. Phys. B (Proc. Suppl.) 136 (2004) 433.
- [8] R.U. Abbasi et al. Phys. Rev. Lett. 92 (2004) 151101.
- [9] M. Takeda et al., Astroparticle Physics 19 (2003) 447462.
- [10] F. Kakimoto et al., Nucl. Instrum. Meth. Phys. Res. A 372 (1996) 527.
- [11] M. Nagano et al. Astropart. Phys. 20 (2003) 293.
- [12] M. Nagano et al. Astropart. Phys. 22 (2004) 235.
- [13] S. Ueno, Master thesis, Tokyo Institute of Technology, 1996 (in Japanese).
- [14] F. Arciprete et al., 29th Int. Cosmic Ray Conf. (Pune) 7 (2005) 55.
- [15] Belz et al, Astroparticle Physics 25 (2006) 129.
- [16] F. Blanco et al., 29th Int. Cosmic Ray Conf. (Pune) 7 (2005) 271.
- [17] <http://www.auger.de/events/air-light-03/>
<http://lappweb.in2p3.fr/IWFM05/>
- [18] B. Keilhauer et al., "Impact of Varying Atmospheric Profiles on Extensive Air Shower Observation: Fluorescence Light Emission and Energy Reconstruction" Astroparticle Physics (in press), available at astro-ph/0511153.
- [19] V. de Souza et al., Astroparticle Physics 25 (2006) 84.
- [20] M. Inokuti, Rev. Mod. Phys. 43 (1971) 297.
- [21] F.R. Gilmore, R.R. Laher and P.J. Espy, J. Chem. Ref. Data 21 (1992) 1005.
- [22] C.O. Laux and C.H. Cruger, J. Quant. Spectrosc. Radiat. Transfer 48 (1992) 9.

- [23] J. B. Birks, *The theory and practice of scintillation counting* chapter 3, Pergamon Press, (Oxford 1964).
- [24] F. Blanco and F. Arqueros, Phys. Lett A 345 (2005) 355
- [25] F. Blanco et al. (in preparation)
- [26] R. M. Sternheimer et al. Phys. Rev. B 26 (1982) 6067.
- [27] R. Roldan et al., J. Appl. Phys. 95 (2004) 5865.
- [28] A. Williart et al., Chem. Phys. Lett. 375 (2003) 39.
- [29] J.M. Fernandez-Varea et al., Nucl. Instrum. Meth. Phys. Res. A 229 (2005) 187.
- [30] S.M.Seltzer, "Cross Sections for Bremsstrahlung Production and for Electron Impact Ionization", in Monte Carlo Transport of Electrons and Photons, Chapt.4 (T.M.Jenkins et al., eds.)(Plenum Press, N.Y. 1988).
- [31] S. T. Perkins et al., "Tables and Graphs of Electron-Interaction Cross Sections from 10 eV to 100 GeV Derived from the LLNL Evaluated Electron Data Library (EDDL)", UCRL-50400 Vol. 31 (November 1991).
- [32] R.M. Sternheimer et al., At. Data and Nucl. Data Tables 30 (1984) 262; W.R. Leo, "Techniques for Nuclear and Particle Physics Experiments", (Springer-Verlag, Berlin 1994).
- [33] <http://physics.nist.gov/PhysRefData/Star/Text/ESTAR.html>
- [34] W.L. Borst and E.C. Zipf, Phys. Rev. A 3 (1970) 834.
- [35] P.N. Stanton and R.M. St. John, J. Opt. Soc. Am. 59 (1969) 252.
- [36] J.F.M. Aarts et al., Physica 40 (1968) 197.
- [37] B.N. Srivastava and I.M. Mirza, Phys. Rev. 168 (1968) 86.
- [38] R. F. Holland, LASL Report No. LA-3783, 1968 (unpublished).
- [39] J.W.McConkey and I.D.Latimer, Proc.Phys.Soc. London 86 (1965) 463.
- [40] J.W.MacConkey, J.M.Woolsey and D.J.Burns, Planet Space Sci. 15 (1967) 1332.
- [41] F. Arqueros et al. An. Fis. 73 (1976) 124 (in Spanish).
- [42] R. O'Neil and G. Davidson, American Science and Engineering, Inc., Rep. AFCRL-67-0277, Cambridge, Mass. (1968)
- [43] G. Davidson and R. O'Neil, J. Chem. Phys. 41 (1964) 3946.
- [44] M.N. Hirsh, E. Poss, P.N. Eisner, Phys. Rev. A 1 (1970) 1615.
- [45] J.T. Fons et al., Phys. Rev. A 53 (1996) 2239.

- [46] D. E. Shemansky and A. L. Broadfoot, *J. Quant. Spectrosc. Rad. Transf.* 11 (1971) 1401.
- [47] M. Imami and W.L. Borst, *J. Chem. Phys.* 61 (1974) 1115.
- [48] D. Rapp and P.Englander-Golden, *J. Chem. Phys.* 43 (1965) 1464; B.L.Schram et al., *Physica* 31 (1965) 94.
- [49] K.B. Mitchell, *J. Chem. Phys.* 53 (1970) 1795.
- [50] M. Nakamura et al., *J. Chem. Ref. Data* 15 (1986) 985
- [51] B. Van Zyl and W. Pendleton, *J. Geophys. Res.* 100 (1995) 23??
- [52] Becker et al. *Chem. Phys. Lett.* 51 111 (1977)
- [53] T. W. Carr and S. Dondes, *J. Phys. Chem.* 81 (1977) 2225
- [54] P. Millet et al., *J. Chem. Phys.* 58 (1973) 5839
- [55] J. M. Calo and J. R. Axtmann, *J.Chem. Phys.* 54 (1971) 1332
- [56] Nichols and Wilson, *Appl. Opt.* 7, 167 (1968)
- [57] V. V. Urosevic et al., *Z.Phys.A - Atoms and Nuclei* 309 (1983) 293.
- [58] M. Simek et al., *J. Phys. D: Appl. Phys.* 35 (2002) 1981.
- [59] S. V. Pancheshnyi et al., *Chemical Physics* 262 (2000) 349.
- [60] A. Morozov, et al., *Eur. Phys. J. D* 33 (2005) 207.
- [61] C. H. Chen et al., *J. Chem. Phys.* 65 (1976) 3863.
- [62] E. Gat et al., *Chem. Phys. Lett.* 306 (1999) 263.
- [63] F. Albugues et al., *J.Chem.Phys.* 61 (1974) 2695.